

# Thioalkanoates as Site-Directing Nucleating Centers for the Preparation of Patterns of CdS Nanoparticles within 3-D Crystals and LB Films of Cd Alkanoates

Shouwu Guo,<sup>‡</sup> Leandro Konopny,<sup>‡</sup> Ronit Popovitz-Biro,<sup>‡</sup> Hagai Cohen,<sup>‡</sup> Horia Porteanu,<sup>§</sup> Efrat Lifshitz,<sup>§</sup> and Meir Lahav<sup>\*,‡</sup>

Contribution from the Department of Materials and Interfaces, Chemical Service Unit, Weizmann Institute of Science, 76100 Rehovot, Israel, and Department of Chemistry and Solid State Institute, Technion, 32000 Haifa, Israel

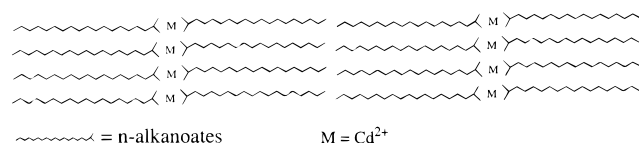
Received April 26, 1999

**Abstract:** A method is described for the preparation of hybrid organic/inorganic structures where the inorganic component comprises semiconductor nanoparticles aligned in periodic layers within three-dimensional (3-D) crystalline powders and Langmuir–Blodgett (LB) films. The preparation process comprises the organization of metal ions in the form of periodic arrays within 3-D crystals or the LB films, followed by a topotactic gas/solid reaction. The method is illustrated for the organization of CdS nanoparticles within alkanolic acids. The order of the nanoparticles is achieved by introducing site directing nucleation centers of Cd thioalkanoates within Cd alkanoates, in the form of solid solutions. The formed particles are attached to the organic matrix via  $-C(O)S-Cd-S-$  bonds. The structure of those supramolecular architectures has been characterized by a variety of complementary methods, including transmission electron microscopy (TEM) and electron diffraction (ED), X-ray powder diffraction (XRD), X-ray photoelectron spectroscopy (XPS), and other spectroscopic measurements.

## Introduction

The design of novel inorganic/organic composite materials, where the inorganic component forms periodic patterns within the organic host matrix, is a major objective in the materials sciences. Of particular interest is the development of new synthetic methodologies for the preparation of systems where the inorganic particles are in the quantum regime with a high degree of monodispersity. As a result of the organization, such materials might display variable optoelectronic properties that differ from those of the isolated particles.<sup>1</sup> In recent years, various strategies have been followed including reactions in reversed micelles,<sup>2</sup> organization of monodispersed quantum particles in organic and biological polymeric templates,<sup>3–8</sup> or

## Scheme 1. Schematic Packing Arrangement of 3-D Crystals and LB Films of Cadmium Alkanoates



specific interactions of the inorganic particles with bolaamphiphilic aromatic molecules.<sup>9</sup>

Here we describe a synthetic strategy that comprises two major steps: selection of 3-D crystals or crystalline ultrathin films of organometallic systems of desired architectures, followed by a topotactic reaction of these solids with a gas.<sup>10,11</sup> Such reactions might yield quantum size particles arranged in patterns, provided the inorganic particles preserve partially the periodic order of the reactant matrix. Furthermore, by selecting the alkanolic acid with the appropriate chain length, one can determine the spacing between the layers of the quantum particles. The preparation of such patterns requires a control over the chemical reactivity of the ions with the gas, a mass transport of the inorganic molecules via anisotropic diffusion within the organic matrix, and finally, the nucleation of the particles at desired sites within the reactant phase. This method was successfully applied for the preparation of quantum size disks of lead sulfide arranged in layers within the organic matrix

<sup>‡</sup> Department of Materials and Interfaces, Weizmann Institute of Science.

<sup>‡</sup> Chemical Service Unit, Weizmann Institute of Science.

<sup>§</sup> Department of Chemistry and Solid State Institute, Technion.

(1) (a) Heitmann, D.; Kottaus, J. P. *Phys. Today* **1993**, *46* (6), 56. (b) Fendler, J. H. *Nanoparticles and nanostructured films: preparation, characterization and applications*; Wiley-VCH: Weinheim, 1998.

(2) (a) Motte, L.; Billoudet, F.; Pileni, M. P. *J. Phys. Chem.* **1995**, *99*, 16425. (b) Motte, L.; Billoudet, F.; Douin, J.; Pileni, M. P. *J. Phys. Chem. B* **1997**, *101*, 138.

(3) Wang, Z. L. *Adv. Mater.* **1998**, *10*, 13.

(4) (a) Braun, P. V.; Osenar, P.; Stupp, S. I. *Nature* **1996**, *380*, 325. (b) Osenar, P.; Braun, P. V.; Stupp, S. I. *Adv. Mater.* **1996**, *8*, 1022.

(5) Shenton, W.; Pum, D.; Sleytr, U. B.; Mann, S. *Nature* **1997**, *389*, 585.

(6) Murray, C. B.; Kagan, C. R.; Bawendi, M. G. *Science* **1995**, *270*, 1335.

(7) Mirkin, C. A.; Letsinger, R. L.; Mucic, R. C.; Storhoff, J. J. *Nature* **1996**, *382*, 607.

(8) Alivisatos, A. P.; Johnsson, K. P.; Peng, X.; Wilson, T. E.; Loweth, C. J.; Bruchez, M. P., Jr.; Schultz, P. G. *Nature* **1996**, *382*, 609.

(9) Andres, R. P.; Bielefeld, J. D.; Henderson, J. I.; Janes, D. B.; Kolagunta, V. R.; Kubiak, C. P.; Mahoney, W. J.; Osifchin, R. G. *Science* **1996**, *273*, 1690.

(10) For reactions of layered metal phosphonates in the solid phase with gaseous  $H_2S$  and  $H_2Se$  see: Cao, G.; Rabenberg, L. K.; Nunn, C. M.; Mallouk, T. E. *Chem. Mater.* **1991**, *3*, 149.

(11) (a) Guo, S.; Popovitz-Biro, R.; Weissbuch, I.; Cohen, H.; Hodes, G.; Lahav, M. *Adv. Mater.* **1998**, *10*, 121. (b) Guo, S.; Popovitz-Biro, R.; Arad, T.; Hodes, G.; Leiserowitz, L.; Lahav, M. *Adv. Mater.* **1998**, *10*, 657.

**Scheme 2.** Schematic Packing Arrangement of Mixed Crystals of Cadmium Alkanoates with Thioalkanoates and the Proposed Nucleation Centers for CdS during the Reactions of These Mixed Crystals with Dry H<sub>2</sub>S

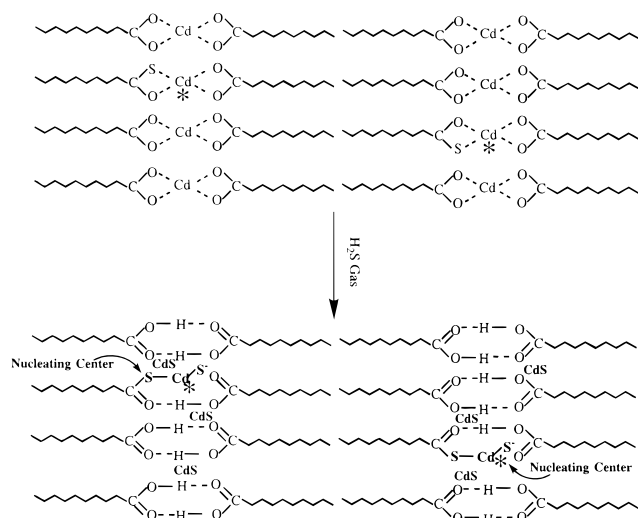


**Table 1.** Layer Spacings of Cd Ions (Å) within Crystals of Cadmium Alkanoates and Thioalkanoates As Determined by XRD

C <sub>n</sub>	C <sub>16</sub>	C <sub>18</sub>	C <sub>22</sub>	C <sub>26</sub>	C <sub>30</sub>
alkanoic	45.32	50.48	59.53	69.50	79.51
thioalkanoic	42.43	46.50	56.35	65.40	76.45

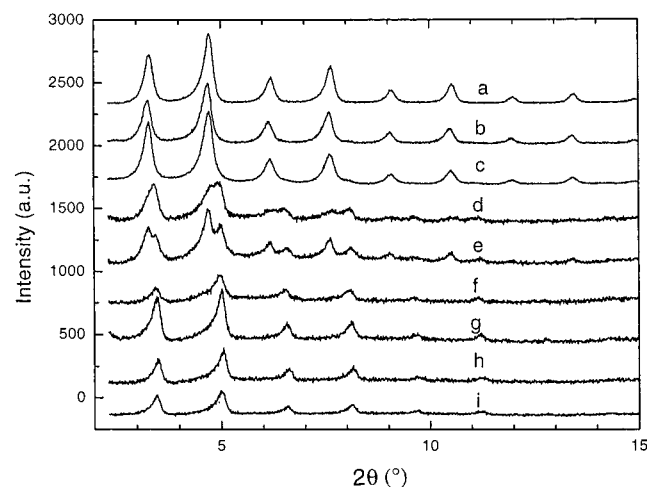


**Figure 1.** XRD patterns of (a) cadmium pure C<sub>22</sub> alkanooate, mixed crystals (solid solutions) containing (b) 10%, (c) 20%, (d) 30%, (f) 50%, (g) 70%, and (h) 90% of the corresponding C<sub>22</sub> thioalkanoate, (e) 1:1 solid mixture, and (i) pure thioalkanoate.

of the fatty acids by reacting powders of lead alkanooates [CH<sub>3</sub>-(CH<sub>2</sub>)<sub>n</sub>-COO]<sub>2</sub>Pb (*n* = 16–28) with H<sub>2</sub>S.<sup>11b</sup> On the other hand, cadmium, zinc, and manganese alkanooates with similar layer structures yield particles randomly arranged or do not react upon treatment with H<sub>2</sub>S. Therefore, the formation of superlattices in systems undergoing reaction depends on the ability to control the size of the particles and the sites where they nucleate. This goal can be achieved by introducing efficient site directing nucleation centers for the inorganic particles at desired loci within the reactant matrix. The approach is illustrated here for the preparation of superlattices of CdS quantum particles within 3-D crystals and Langmuir–Blodgett (LB) films of Cd alkanooates upon their reaction with H<sub>2</sub>S, using the thioalkanoates as the site directing nucleating species.

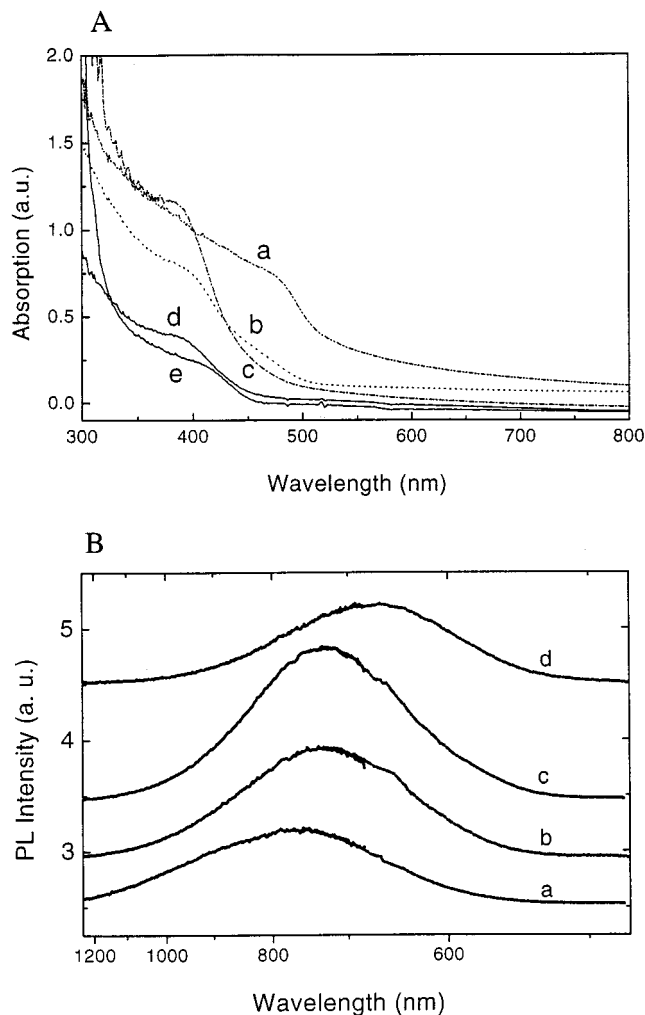


**Figure 2.** (A) UV-vis absorption spectra of CdS particles generated within (a) C<sub>16</sub>, (b) C<sub>18</sub>, (c) C<sub>22</sub>, (d) C<sub>26</sub>, and (e) C<sub>30</sub> cadmium alkanooate matrices after completion the reaction with dry H<sub>2</sub>S and extracted in DMSO. (B) Photoluminescence spectra of CdS particles generated in the (a) C<sub>16</sub>, (b) C<sub>18</sub>, (c) C<sub>22</sub>, and (d) C<sub>30</sub> cadmium alkanooate matrices, measured directly on the reacted powders.

**Selection of the Model.** Schematic packing arrangements of the homologous series of Cd alkanooates crystals or LB films are shown in Scheme 1. The Cd ions within these crystals or LB films form 2-D layers that are separated from one another by a spacing that is twice that of the length of the hydrocarbon chains. Consequently, the spacing between these layers can be altered just by selecting the acid with the appropriate hydrocarbon chain length. Upon reaction of the crystallites with H<sub>2</sub>S, CdS molecules are generated, which have a strong tendency to crystallize as particles. The diffusion of the CdS molecules prior to crystallization within the organic matrix is expected to be anisotropic. One may anticipate the formation of CdS particles aligned in layers provided the CdS molecules nucleate preferentially within the hydrophilic layers where the Cd ions reside. Results on the Cd salts of the common fatty acids, such as stearic (C<sub>18</sub>), behenic (C<sub>22</sub>), and hexacosanoic (C<sub>26</sub>) acid, were disappointing since the CdS particles were either substantially large or randomly distributed within the organic matrix. Enhanced nucleation of the particles along the ionic rows can be achieved by introducing, regioselectively, nucleating centers along the hydrophilic layers of the reactant. Thus, for example, Cd thioalkanoates of the same chain lengths should be easily dissolved within the corresponding Cd alkanooates to form

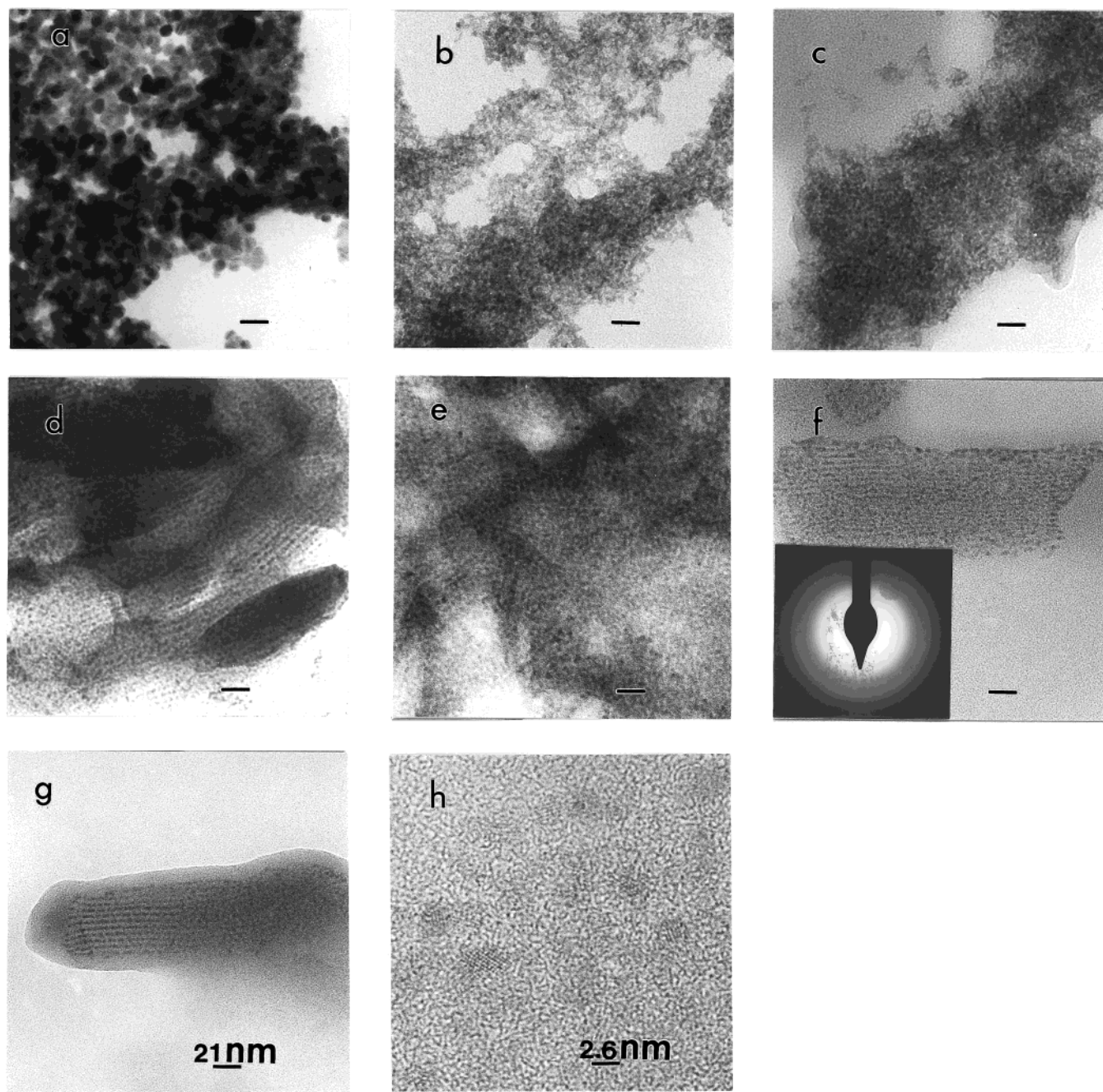


**Figure 3.** (a–d) TEM images of CdS particles generated within pure  $C_{16}$ ,  $C_{22}$ ,  $C_{26}$ , and  $C_{30}$  cadmium alkanoate matrices, respectively. (e–g) TEM images of CdS particles generated in the mixed crystals of Cd  $C_{16}$ , Cd  $C_{22}$ , and Cd  $C_{26}$  alkanoates containing 10% of the corresponding Cd thioalkanoate. Insert in panel f shows selected area electron diffraction of CdS particles formed within the Cd  $C_{22}$  alkanoate/10% Cd  $C_{22}$  thioalkanoate mixed crystal. (h) High-resolution TEM images of CdS particles shown in panel g. Images a–g were taken at the same magnification.

random solid solutions and thus assuming the conformation and tilt angle of the chains of the molecules in the host crystal. Powders of the pure Cd thioalkanoates, with related crystal structures to those of the alkanoate salts, react very slowly, if at all, with dry  $H_2S$  and so are designated as an “inert pair”.<sup>12</sup> Within the mixed crystals, one may foresee the formation of a Cd carboxylates pair and a mixed pair of two components. For the low concentrations, the number of inert thiocarboxylates pairs would be small, as shown in Scheme 2. Consequently, in the mixed crystals the Cd carboxylates pairs are expected to react as in their pure salts to yield the CdS molecules, while the Cd ions of the mixed pairs react with  $H_2S$  at the  $-COOCd$

only, but not at the  $-C(O)SCd$  sites. Upon such reaction the CdS molecules formed at the carboxylates sites diffuse and nucleate at the nearest  $-C(O)SCd$  sites that are bound to the organic matrix, resulting in the formation of layers of CdS nanoparticles, within the hydrophilic layers of the reactant crystals. These patterns should be preserved provided that the fatty acid formed after reaction does not recrystallize. Furthermore, by adjusting the concentration of the thioalkanoates in the mixed crystals one should be able to control, albeit within limits, the number of nucleating centers and consequently the size of the inorganic crystallites.

#### Experimental Section

**I. Materials.** Cadmium chloride ( $CdCl_2$ ), sodium sulfide ( $Na_2S$ ), sulfuric acid ( $H_2SO_4$ ), potassium hydroxide (KOH), phosphorus pen-

(12) The reactivity with wet  $H_2S$  occurs at a moderate rate due to some hydrolysis.<sup>13</sup>

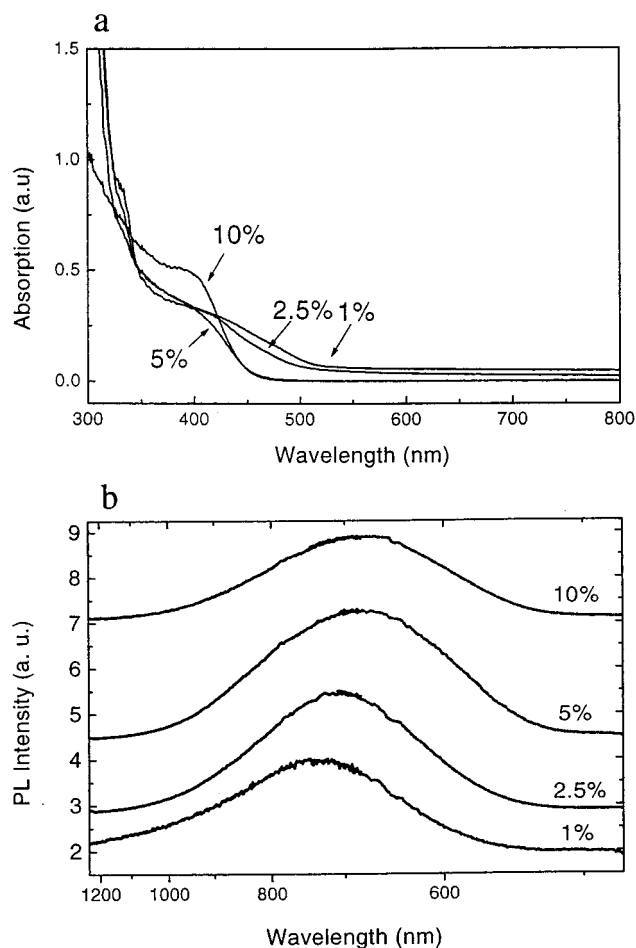


**Figure 4.** (a) UV-vis absorption spectra of CdS particles generated within Cd C<sub>18</sub> mixed crystals containing 1%, 2.5%, 5%, and 10% corresponding thioalkanoates that were measured after extracted in DMSO suspensions. (b) Photoluminescence spectra of the corresponding CdS particles, measured directly in the solid state at 77 K within reacted powders.

toxide (P<sub>2</sub>O<sub>5</sub>), methanol, ethanol, dimethyl sulfoxide (DMSO) (Merck), and alkanolic acids CH<sub>3</sub>(CH<sub>2</sub>)<sub>n</sub>COOH (*n* = 14–28) (Sigma) were used without additional purification.

The thioalkanoic acids were synthesized through the reactions of KSH with acyl chlorides of the corresponding alkanolic acids.<sup>14</sup> The acyl chlorides were prepared by the reaction of the fatty acids with POCl<sub>3</sub>. KSH was prepared by bubbling H<sub>2</sub>S gas through an ethanolic solution of KOH. The purity of the thioalkanoic acids was demonstrated, selectively shown here for CH<sub>3</sub>(CH<sub>2</sub>)<sub>20</sub>COSH (molecular weight *M* = 356), by mass spectrometry (*m/e* 357); NMR (CDCl<sub>3</sub>) δ 0.96 (t, 3H), 1.33 (m, 38H), 2.68 (t, 3H); IR (KBr) 2929, 2851, 2557, 1676, and 1472 cm<sup>-1</sup>. The thioalkanoic acids were converted into the more stable corresponding potassium salts and stored as such at -5 °C. The Cd salts of the acids and the mixed crystals were prepared by mixing ethanol solutions of the corresponding potassium salts with aqueous solution of CdCl<sub>2</sub>.

H<sub>2</sub>S (g) was either prepared through the reaction of Na<sub>2</sub>S with 20% H<sub>2</sub>SO<sub>4</sub> and used without drying (hereafter wet H<sub>2</sub>S) or taken from commercial cylinders (Merck) and used after drying by passing it through a tube of P<sub>2</sub>O<sub>5</sub> (hereafter dry H<sub>2</sub>S). The gas-solid reactions were performed at room temperature (25 °C).

The Langmuir films were prepared by spreading 10<sup>-3</sup> M chloroform solutions of the alkanolic acids or chloroform (mixed with 5% of ethanol) solutions of the mixtures of alkanolic acids with a certain

percent of the corresponding potassium thioalkanoates on the aqueous solution of CdCl<sub>2</sub> at pH 7.2. The films were transferred onto solid supports by the vertical dipping method on a Lauda FW-2 trough.

**II. Characterization Methods.** FT-IR spectra of the 3-D crystal powders were measured in KBr pellets on a Nicolet-460 spectrometer. LB films were deposited on CaF<sub>2</sub> slides and the FT-IR spectra were measured.

UV-vis absorption spectra of the CdS nanoparticles after extraction from the reacted powders were recorded on a Beckman DU-7500 spectrometer. The spectra of the LB films were measured after deposition on glass slides.

TEM images and ED patterns were taken on a Philips CM12 transmission electron microscope operated at 100 kV or a Philips CM120 transmission electron microscope operated at 120 kV. The composite 3-D crystallites, after completion of the reaction with H<sub>2</sub>S, were placed on collodion/carbon 400 mesh electron microscope grids from sonicated 1:1 water-ethanol suspension, which were blotted after 30 s. LB films for TEM experiments were deposited on collodion/carbon coated nylon grids (inert to H<sub>2</sub>S gas) which were attached to glass slides for the dipping procedure and then reacted with H<sub>2</sub>S on the grids. Images of these films were taken at -170 °C (using a Gatan cold stage) under low-dose conditions.

The X-ray powder diffraction patterns were recorded on a Rigaku RU-200B rotax diffractometer using Cu Kα λ = 1.54 Å.

XPS measurements were performed on a Kratos AXIS HS instrument, using a monochromatized Al (Kα) source and a 20 eV pass energy. Though energy resolution was limited to about 0.5 eV, the accuracy (and stability) of the energy scale enabled determination of peak relative positions within ±0.05 eV. For final calibration of the energy scale, the main C (1s) peak was set to 284.8 eV. Special care has been taken to diminish the beam-induced damage, found to be nonnegligible on time scales of about 1 h. To obtain nondamaged reliable spectra, low-power radiation was used (5 mA emission at 15 kV). Evolution of spectra measured at a fixed spot was first studied, yielding the relevant time scale for "fresh area" data recording, and providing the information required for extrapolations (to zero radiation time) in the analysis of element concentrations and line shapes. The present results account for 5–10 min exposure time or 20 min at most. Curve-fitting analysis of line shapes was performed with Vision software, using Shirley background subtraction and Gaussian-Lorentzian line shapes. The spectra of the LB films were taken on glass slides.

The photoluminescence spectra were recorded by immersing the sample in a variable-temperature 12CNDT Janis cryogenic Dewar. The spectra were obtained by exciting the sample with a continuous 457.9 nm Ar<sup>+</sup> laser (Coherent, Innova 90). The transmitted or emitted light passed through a holographic grating monochromator (Acton Model SpectraPro 300) and was detected by an ICCD camera (PI model 576).

## Results and Discussions

**I. Topotactic Gas/Solid Reactions in 3-D Crystalline Powders.** The homologous series of cadmium C<sub>16</sub>, C<sub>18</sub>, C<sub>22</sub>, C<sub>26</sub>, and C<sub>30</sub> alkanooates, thioalkanoates, and their mixtures were prepared and characterized by XRD and FT-IR spectra. The spacings between the Cd ion layers in the different crystals are listed in Table 1.

XRD patterns of Cd C<sub>22</sub> alkanooate and thioalkanoate are shown in Figure 1a, i. These patterns indicate that the Cd ions within these powders are arranged in layers that are separated by a spacing that is twice the length of the corresponding hydrocarbon chain in the extended conformation (see Scheme 1). The packing arrangements of the thioalkanoates are very similar to those of the corresponding alkanooates, with the exception that the spacing between the Cd ion layers is somewhat shorter. It implies that the hydrocarbon chains in these crystals are tilted about 20° off the normal to the plane. The difference in organization arises from the binding of the Cd ions in the two systems. In the alkanooates, the Cd ions are bound equally to two oxygen atoms, as deduced from the XPS data, as well as from the asymmetric carboxylate stretching vibration

(13) Tao, Y.; Pandiaraju, S.; Lin, W.; Chen, L. *Langmuir* **1998**, *14*, 145.

(14) (a) Noble, P., Jr.; Tarbell, D. S. *Organic Syntheses*; Wiley: New York, 1963; Collect. Vol. 4, p 924. (b) Shin, H. C.; Quinn, D. M. *Lipids* **1993**, *28*, 73.

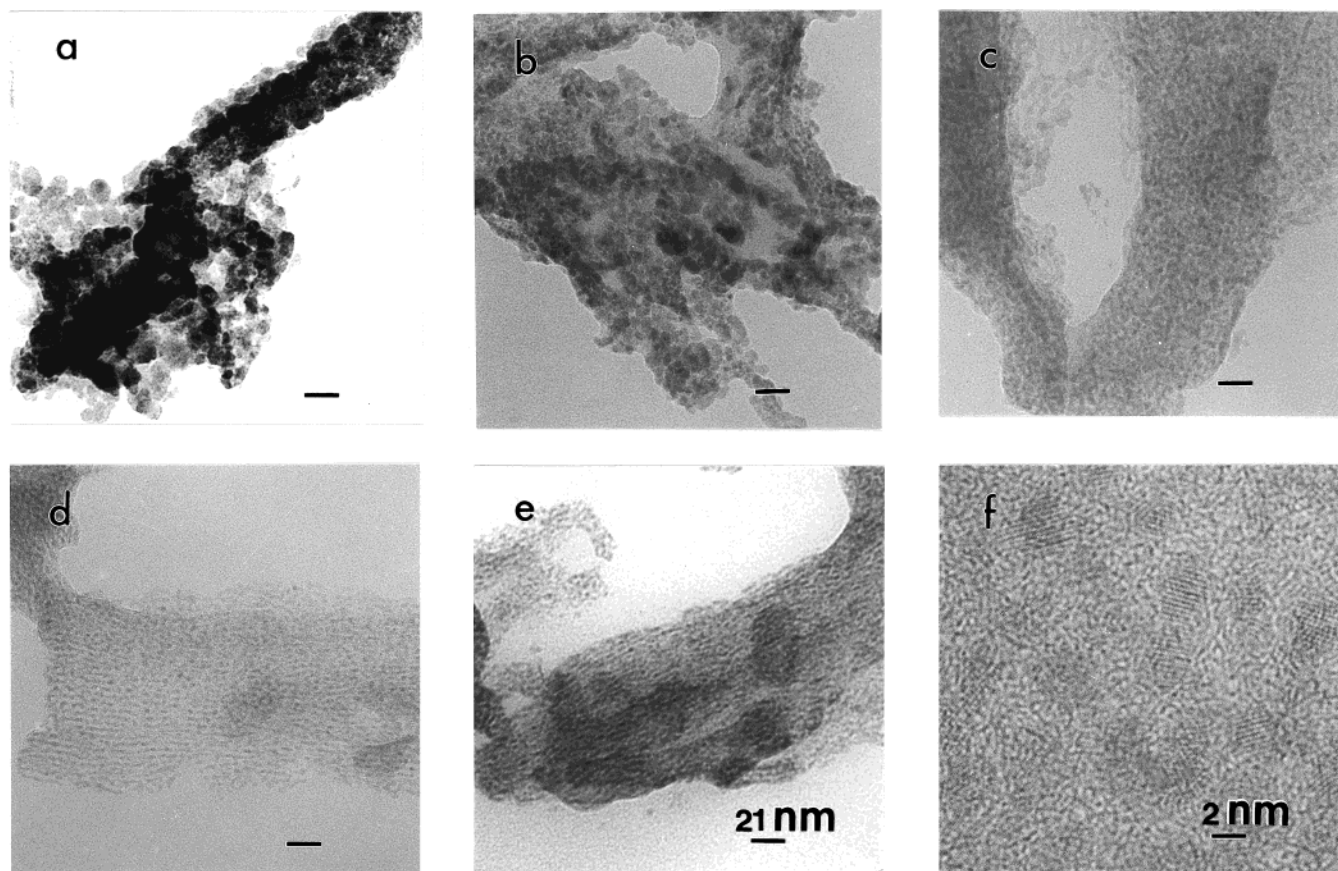


**Figure 5.** TEM images of CdS particles formed in cadmium (a)  $C_{18}$  alkanolate and mixed crystals containing (b) 1%, (c) 2.5%, (d) 5%, and (e) 10% of  $C_{18}$  thioalkanoate. (f) High-resolution TEM images of the cubic CdS particles shown in panel d. Images a–e were taken at the same magnification.

band at  $1542\text{ cm}^{-1}$  in the FT-IR spectra. On the other hand, in the thioalkanoate, the Cd ions are bound preferentially to the sulfur atoms. The latter was concluded from XPS data and the appearance of the IR stretching band at  $1656\text{ cm}^{-1}$ , assigned to a carbonyl bond, and from the absence of a band at  $1150\text{ cm}^{-1}$ , due to the C=S bond<sup>15</sup>.

Powders of the pure Cd alkanolates were exposed to dry  $H_2S$  at atmospheric pressure, yielding CdS particles and centrosymmetric pairs of the alkanolic acids, as followed from the replacement of the carboxylate stretching band at  $1542\text{ cm}^{-1}$  by that of the carbonyl at  $1705\text{ cm}^{-1}$  in the FT-IR spectrum.<sup>16–17</sup> After completion of the reaction, the CdS particles were extracted in DMSO using 3-mercapto-1,2-propanediol as a stabilizer. The UV–vis absorption spectra of the CdS particles, generated in the different salts, are shown in Figure 2A. The absorption onsets of the CdS particles generated within  $C_{16}$  and  $C_{18}$  are at 520 nm or above, and correspond to relatively large CdS particles. On the other hand, the absorption onsets of the particles formed within  $C_{22}$ ,  $C_{26}$ , and  $C_{30}$  are blue shifted to 470, 460, and 455 nm, respectively, indicating that the particles are quantum sized.<sup>18</sup> A pronounced blue shift is also recognized in the photoluminescence (PL) spectra of CdS particles within the alkanolates, as presented in Figure 2B. Those spectra consist of a relatively broad emission band that is Stokes shifted from

the absorption edge by about 25 nm. Moreover, those bands show a radiative lifetime of a microsecond and a multiexponential decay process (not shown). Bawendi et al.<sup>19</sup> showed that interparticle interactions within a self-assembled periodic structure cause a red shift of an exciton of about 2 nm, with respect to that of an individual particle, and also shorten the exciton lifetime in the nanosecond time range. Thus, interparticle interactions alone will not explain the substantially larger Stokes shift and the long lifetime in our case. Instead, it may indicate that this band is not excitonic, and rather corresponds to a defect recombination process. Despite the deepness of the luminescence band, it shows a pronounced blue shift with a decrease in particle size. This indicates that at least one of the recombining defect sites has a shallow state that manages to follow the quantization effect of the adjacent band edge.<sup>20,21</sup> Figures 3a–d and 5a show the bright field TEM images of the Cd alkanolate powders after completion of the reaction with  $H_2S$ . In agreement with the UV–vis measurements, the particles generated within  $C_{16}$  and  $C_{18}$  are substantially large, over 100 Å in diameter (Figures 3a and 5a). The particles formed within the  $C_{22}$  and  $C_{26}$  (Figure 3b,c) are smaller, 20–40 Å in diameter, but still randomly distributed in the matrices. The particles generated within crystals of  $C_{30}$  are not only small, with a size range of 20–30 Å in diameter, but also arranged in discrete layers within the crystals (Figure 3d).

Summarizing the reactivity in these related systems, one finds a correlation between the spatial separation of the ion layers in the reactant phase (as determined by the hydrocarbon chain

(15) In the FT-IR spectra of the corresponding potassium thioalkanecarboxylates, the C=S stretching band at  $1150\text{ cm}^{-1}$  was observed implying that the  $K^+$  ion is attached to the oxygen.

(16) Holland, R. F.; Nielsen, J. R. *J. Mol. Spectrosc.* **1962**, *9*, 436.

(17) Dote, J. L.; Mowery, R. L. *J. Phys. Chem.* **1988**, *92*, 1571.

(18) Wang, Y.; Suna, A.; Mahler, W.; Kasowski, R. *J. Chem. Phys.* **1987**, *87*, 7315.

(19) Kagan, C. R.; Murry, C. B.; Bawendi, M. G. *Phys. Rev. B* **1996**, *54*, 8633.

(20) Lifshitz, E.; Dag, T.; Litvin, I. D.; Hodes, G.; Roisfeld, R.; Zelman, M.; Minti, H. *Chem. Phys. Lett.* **1998**, *288*, 188.

(21) Lifshitz, E.; Litvin, I. D.; Porteanu, H.; Lipovskii, A. A. *Chem. Phys. Lett.* **1998**, *295*, 249.

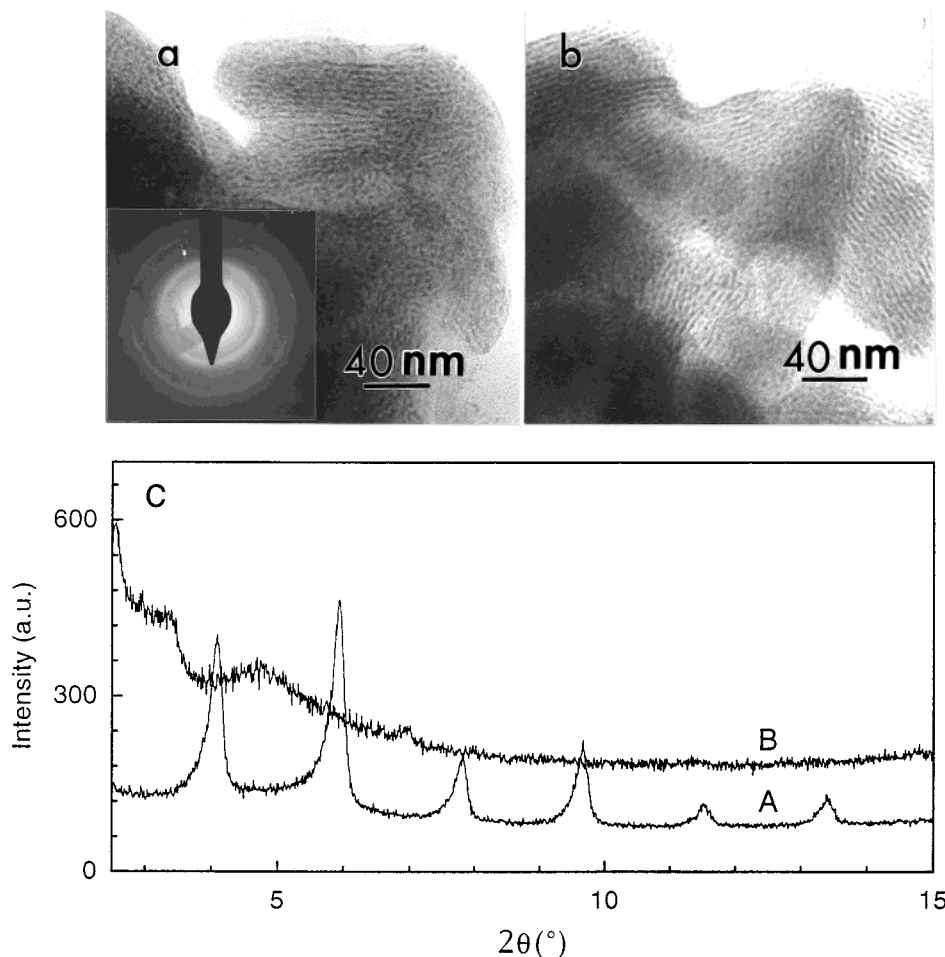


**Figure 6.** (a, b) TEM images CdS particles formed within cadmium C<sub>18</sub> alkanooates containing 50% and 70% of the corresponding thioalkanoates after exposure to dry H<sub>2</sub>S for 7 h, respectively. Insert in panel a shows selected area electron diffraction of the CdS particles. (c) XRD patterns of Cd C<sub>18</sub> alkanooate containing 50% of the corresponding thioalkanoate (A) before and (B) after exposure to dry H<sub>2</sub>S for 7 h.

length) and the size and organization of the resultant CdS particles. When the ion layers are separated by a distance of 40–50 Å, the CdS particles are large and randomly distributed; when the layer spacing is 60–70 Å, the particles are small, but still randomly distributed. Finally, the particles are small and arranged in layers when a spacing of 80 Å or more separates the ion layers.

Since Cd alkanooate and thioalkanoate have similar structures, solid solutions of the two could be formed, as suggested in Scheme 2. Three different regimes were observed in the solid solutions as shown by the XRD patterns of the C<sub>22</sub> (Figure 1b–d, f–h). In regime I, with nominal concentration of the thioalkanoate lower than 20%, the mixed crystals assume the same packing arrangement as that of the pure alkanooate. In regime II, where the nominal concentration of the thioalkanoates is above 50%, the mixtures precipitate in the same phase as that of the pure thioalkanoate and in this phase the hydrocarbon chains of the alkanooate assume the structure and tilt angle of the thioalkanoate. In regime III, when the concentration of thioalkanoate is 20–50%, two phases are formed.

Mixed crystals of C<sub>16</sub>, C<sub>18</sub>, C<sub>22</sub>, and C<sub>26</sub> containing 10% of the corresponding thioalkanoate, in the alkanooate phase, were exposed to H<sub>2</sub>S to generate CdS particles. The CdS particles in the C<sub>16</sub> mixture are substantially smaller as compared to those generated in the pure alkanooate, but still randomly arranged in the matrix. Within the mixed crystals of C<sub>18</sub>, the average size of the CdS particles is smaller as compared to those generated in the pure alkanooate and, furthermore, the particles are arranged

as periodic layers. For C<sub>22</sub> and C<sub>26</sub>, the particles are 20–30 Å in diameter, with a high degree of alignment. Their TEM images are shown in Figures 3e, 5e, and 3f, g, respectively.

The effect of thioalkanoate concentration within the solid solution on the size and arrangement of the CdS particles was systematically investigated on the C<sub>18</sub> system. Mixed crystals were prepared from solutions containing an increasing percentage of the thioalkanoate. The concentrations of the thioalkanoates in the mixed crystals were determined by elemental analysis, shown in parentheses: 1% (0.67%), 2.5% (2.56%), and 10% (8.83%). Figure 4 shows UV–vis and PL spectra of CdS particles, formed in mixed crystals precipitated from solutions bearing a given percentage of the thioalkanoates. The presence of 1% thioalkanoate does not change the absorption onset of the particles relative to that of the CdS bulk. However, a blue shift is already observed upon increase to 2.5% or above, reaching a plateau with 5% of the thioalkanoate. The absorption onset with 10% thioalkanoate is almost identical with that of the 5% mixture. These conclusions were independently confirmed by PL spectra of the CdS particles recorded within the reacted powders.

Figure 5 shows TEM images of reacted salts of pure Cd C<sub>18</sub> alkanooate and mixtures of the latter with varying amounts (1–10%) of Cd C<sub>18</sub> thioalkanoates. Cubic CdS particles (Figure 5f) of 30–35 Å in diameter are formed. Within powders that contain 5% or more of the thioalkanoate the CdS particles are arranged as periodic layers. The size of the particles, as determined by the TEM measurements, is in agreement with

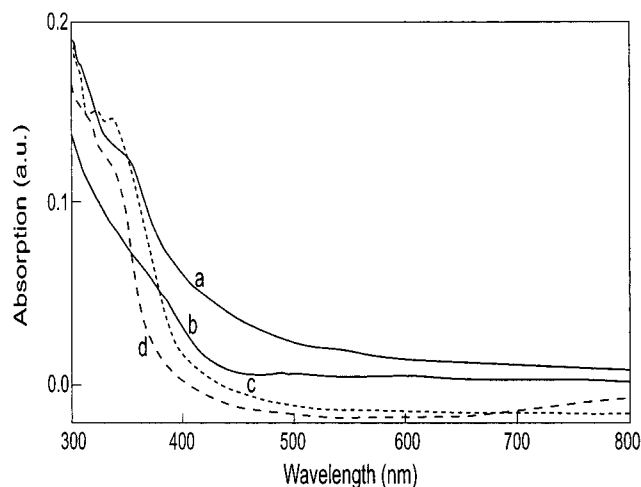
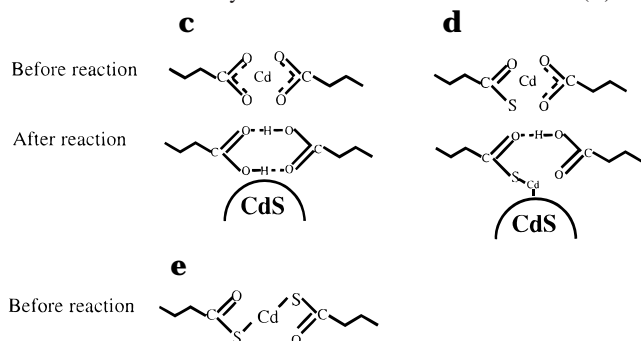


**Figure 7.** UV-vis absorption spectra of LB films of (a) pure Cd C<sub>22</sub> alkanolate and the mixtures containing (b) 10%, (c) 50%, and (d) 80% of the corresponding thioalkanoates after completing the reactions with H<sub>2</sub>S.

**Table 2.** Binding Energies (eV) as Determined by XPS for Oxygen (1s), Carbon (1s), Cadmium (3d<sub>5/2</sub>), and Sulfur (2p<sub>3/2</sub>), Measured in 3-D Crystals and LB Films of Pure Cadmium C<sub>22</sub> Alkanolate and Mixtures with the Corresponding Thioalkanoates

	thioalkanoate related peaks <sup>d</sup>					
	pure alkanolate <sup>c</sup>		low concn <sup>d</sup>		high concn <sup>e</sup>	
	before reaction	after reaction	before reaction	after reaction	before reaction	after reaction
O (1s)	531.45	532.00 533.30	532.00	532.00	532.00	532.30
C (1s)	288.50	289.15	287.00	287.00	287.50	287.50 288.0 <sup>b</sup>
Cd (3d <sub>5/2</sub> )	405.45	405.05			405.55	405.40
S (2p <sub>3/2</sub> )		161.40	162.00	162.40	162.50	162.40 163.80

<sup>a</sup> In the mixed crystals, the carboxylate related peaks appear in addition to the thioalkanoate related ones. <sup>b</sup> Associated with -C(O)SH.



the size deduced from the UV-vis absorption and photoluminescence measurements.

Superlattices of CdS nanoparticles within the reactant matrices were also formed within the thioalkanoate-enriched phases of regime II (Figure 6). The XRD patterns of the crystalline powders after completion of the reaction with H<sub>2</sub>S showed a few new broad peaks (Figure 6c). The low-angle (001) diffraction peak in the product could not be observed on our instrument. The spacings between the layers of particles are larger than those between the ion layers measured in the reactant prior to reaction. This observation implies that the particles are formed within the matrix itself releasing the stress built up during reaction by an expansion of the crystal lattice.

**Table 3.** The Nominal and XPS Determined Thioalkanoate Concentrations in the Mixed Crystals, and the XPS Determined Core and Surface Ratios of Cd and S of the CdS Particles Formed within Different Mixed Crystals

nominal	concn of thioalkanecarboxylate (%)		XPS determined core and surface ratios of Cd and S of CdS particles (%)		
	XPS determined		Cd + S in core	Cd on surface	S on surface
80	67		12	40	48
50	33		40	26	34
10	10		70	20	8
0	0		90	10	<5

**II. Organization of the CdS Nanoparticles in Superlattices within LB Films.** The reactivity of LB films of Cd alkanolates (stearate, arachidate, and behenate) with H<sub>2</sub>S has been overwhelmingly studied over the years.<sup>22-24</sup> Yet an issue that still remains under debate is whether the CdS particles generated within these films are periodically aligned or randomly distributed therein. In some investigations,<sup>25,26,27</sup> researchers had deduced that superlattices of the CdS particles were probably generated. Ordering of the CdS particles within these LB films is difficult to detect by TEM because of an improper orientation of the alkanolic acid layers vis-a-vis the probing electron beam. Recent studies applying Rutherford backscattering measurements on cadmium arachidate LB films composed of 700 layers have demonstrated that the CdS particles were not organized in layers, but are rather distributed randomly within the organic film.<sup>28</sup> These observations are in agreement with the present studies on the 3-D powders of the corresponding Cd alkanolates that assume packing arrangements that are analogous to the LB films. Due to the strong hydrophobic interactions between the hydrocarbon chains, crystalline domains are formed at the water surface, thus limiting the preparation of LB films of Cd alkanolates to hydrocarbon chains up to C<sub>22</sub>.<sup>29</sup> Hence, the method of site directing nucleation should be most appropriate for the preparation of nanoparticle superlattices in such systems.

LB films of Cd alkanolate and thioalkanoate mixtures with different compositions were prepared and deposited on hydrophilic glass slides. Since the thioalkanoates undergo partial hydrolysis on the water surface prior to transfer to the glass, the relative ratios of the alkanolate to thioalkanoate had been predetermined by XPS for each specimen film before reaction. The progress of reaction was monitored by FT-IR and XPS, as for the 3-D crystalline powders. The UV-vis absorption spectra of the LB films of pure Cd C<sub>22</sub> (behenate) and mixtures containing 10%, 50%, and 80% of thiobehenate, after reaction with H<sub>2</sub>S at 25 °C and at atmospheric pressure, are shown in Figure 7. From these spectra, one deduces that by increasing the concentration of the thiobehenate, the absorption onset is blue shifted, implying a decrease in size of the particles. The

(22) Geddes, N. J.; Urquhart, R. S.; Furlong, D. N.; Lawrence, C. R.; Tanaka, K.; Okahata, Y. *J. Phys. Chem.* **1993**, *97*, 13767.

(23) Moriguchi, I.; Hosoi, K.; Nagaoka, H.; Tanaka, I.; Teraoka, Y.; Kagawa, S. *J. Chem. Soc., Faraday Trans.* **1994**, *90* (2), 349.

(24) Urquhart, R. S.; Hoffmann, C. L.; Furlong, D. N.; Geddes, N. J.; Rabolt, J. F.; Grieser, F. *J. Phys. Chem.* **1995**, *99*, 15987.

(25) Smotkin, E. S.; Lee, C.; Bard, A. J.; Campion, A.; Fox, M. A.; Mallouk, T. E.; Webber, S. E.; White, J. M. *Chem. Phys. Lett.* **1988**, *152*, 265.

(26) Pan, Z.; Liu, J.; Peng, X.; Li, T.; Wu, Z.; Zhu, M. *Langmuir* **1996**, *12*, 851.

(27) (a) Basu, J. K.; Sanyal, M. K. *Phys. Rev. Lett.* **1997**, *79*, 4617. (b) Vitta, S.; Metzger, T. H.; Major, S. S.; Dhanabalan, A.; Talwar, S. S. *Langmuir*, **1998**, *14*, 1799.

(28) Yamaki, T.; Asai, K.; Ishigure, K. *Chem. Phys. Lett.* **1997**, *273*, 376.

(29) Zasadzinski, J. A.; Viswanathan, R.; Madsen, L.; Garnæs, J.; Schwartz, D. K. *Science* **1994**, *263*, 1726.

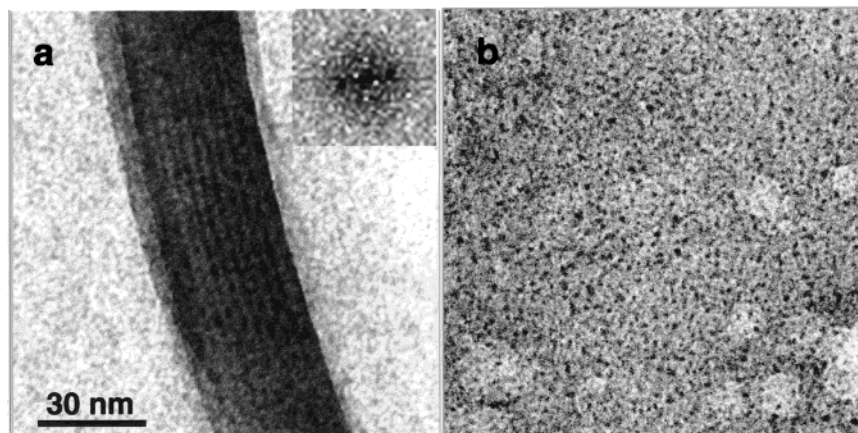


**Figure 8.** TEM images of CdS particles formed in LB films of  $C_{22}$  alkanate containing 50% of the corresponding thioalkanoate (a) and pure Cd  $C_{22}$  alkanate (b). Part a shows a folding in the LB film, revealing both top and side views. The inset shows FFT from the side view region. All images were taken at the same magnification.

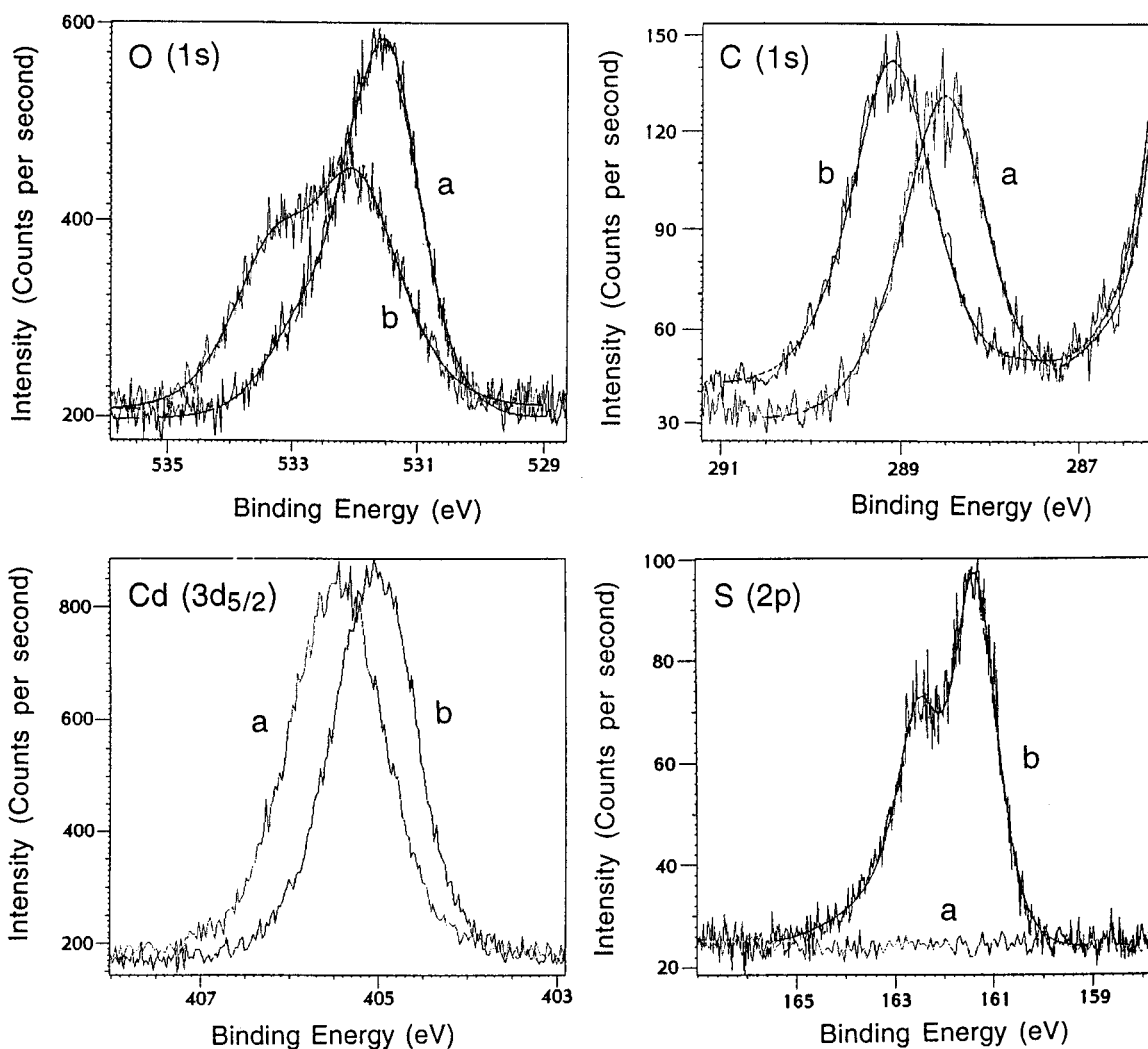


**Figure 9.** XPS spectra of O (1s), C (1s) of carbonyl, Cd (3d<sub>5/2</sub>), and S (2p) in the 3-D crystals and LB films of pure Cd  $C_{22}$  alkanate (a) before and (b) after completion of the reaction with  $H_2S$ .

XPS results are practically identical with those obtained from 3-D crystalline powders as summarized in Table 2 and Figures 9 and 10 (see next paragraph), revealing that part of the CdS nanoparticles are linked directly to the thioalkanoates in the LB films, in agreement with the proposed mechanism. In fact, even narrower XPS lines of the films indicate an overall better homogeneity as compared with the 3-D analogues (Scheme 2). TEM measurements of the LB films, deposited on nylon grids

and reacted with  $H_2S$ , demonstrate that some of the latter had folded on the grid, thus exposing regions in an appropriate orientation vis-a-vis the electron beam. Consequently, periodic order of the CdS nanoparticles could be detected in these regions, as shown in Figure 8. Stripes of disklike CdS particles were observed, 10–20 Å in width and 30–45 Å in length, in agreement with the results obtained in the 3-D crystallites. In contrast, the CdS particles formed in the LB films of the pure



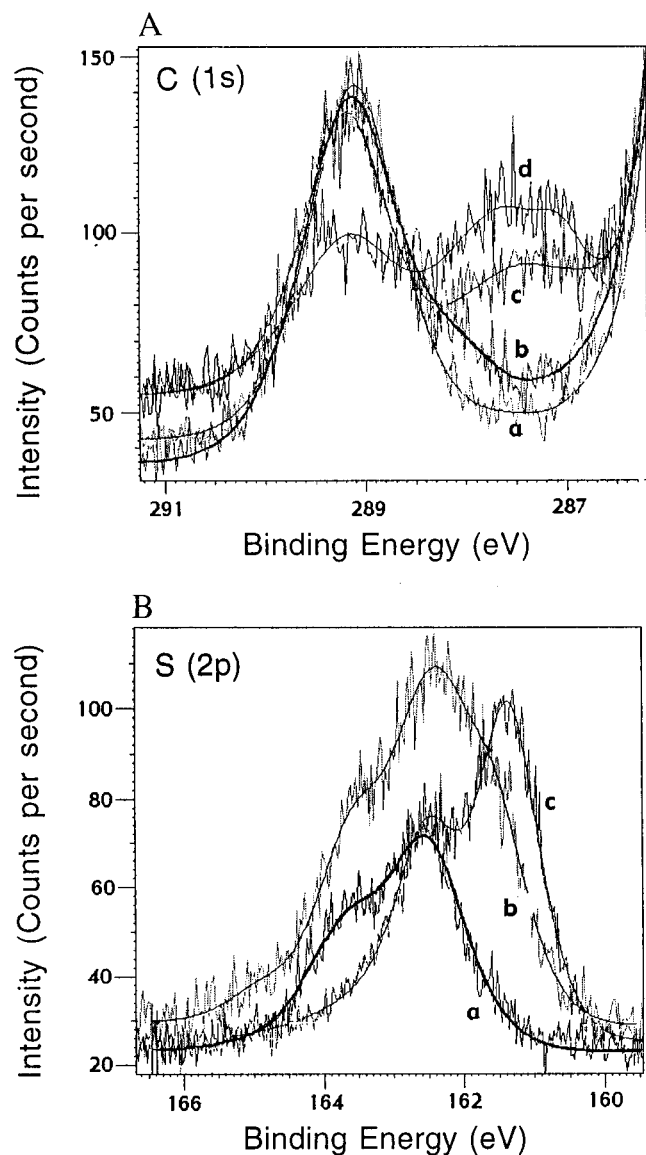


**Figure 10.** (A) XPS spectra of the carbonyl carbon (1s) in (a) pure  $C_{22}$  Cd alkanoate and within mixtures containing (b) 10%, (c) 50%, and (d) 80% of the corresponding thioalkanoate; (B) XPS spectra of S in the mixtures of Cd  $C_{22}$  alkanoate containing (a) 50% of the thioalkanoate before reaction with  $H_2S$  and (b) 80% of thioalkanoate after reaction with  $H_2S$  and (c) XPS spectrum of S in the pure Cd  $C_{22}$  alkanoate after reaction with  $H_2S$ .

Cd behenate are randomly distributed with an average diameter of  $40 \text{ \AA}$ , consistent with the Rutherford backscattering observations.<sup>28</sup>

**III. XPS of Cd  $C_{22}$  Matrices.** Binding energies and the lines of the various elements, C (1s), O (1s), Cd (3d), and S (2p), provided a rather complete picture of the headgroups structures, both in the powders and in the LB films. The binding energies, listed in Table 2, were calibrated for a backbone carbon peak at 284.8 eV. As shown in Figure 9, assignment of the pure alkanoates XPS lines is relatively straightforward. Before reaction, a single chemical state for the Cd ( $3d_{5/2}$ ) (405.45 eV) is suggested by the relatively narrow lines, while the carbon signal of the carboxylate at 288.5 eV reflects high homogeneity of the studied material. Upon sulfidation, these lines exhibit a clear chemical shift (to 405.05 and 289.15 eV, respectively). The small shift of the Cd line (accompanied by the appearance of a sulfur line) is in full agreement with the formation of CdS particles. The observed carbon signal at 289.15 eV in the reacted

sample is attributed to that of the pure carboxylic acid (a value verified by a reference sample). Correspondingly, before reaction the O (1s) line shows a dominant signal at 531.45 eV, reflecting the equal role of the four oxygen atoms in the carboxylates Cd complex. After a reaction, the O (1s) peaks at 532.0 and 533.3 eV are assigned to the oxygen of carbonyl (C=O) and the oxygen of the hydroxide in the  $[-C(O)-OH]$ , respectively. (It is noted that at low intensity, additional oxygen signals are always detected, as discussed below.)

Analysis of the mixed crystals comprising the thioalkanoates demonstrates evolution of new peaks (see Table 2 and Figure 10). The carbon signal of the thiocarboxylate group at 287.5 eV is found to increase with an increase of the concentration of the thioalkanoates (before reaction); however, not in a simple linear manner. We also noticed a shift from 287.0 eV (low concentrations of thioalkanoate, namely thio-diluted) to 287.5 eV (high concentrations of thioalkanoate, namely thio-rich). This difference in energies (see Table 2), is attributed to the formation of different pairs around the Cd ions: thiocarboxylate/carboxylate or thiocarboxylate/thiocarboxylate. After sulfidization, these lines are slightly modified, depending on the concentration of the thioalkanoate, unfolding into three overlapping contributions determined at 287.0, 287.5, and 288.0 eV. The latter component is associated with "free"  $-C(O)S-H$  groups as verified from the appearance of the corresponding S ( $2p_{3/2}$ ) signal at 163.8 eV.

Accordingly, before reaction with  $H_2S$ , the S ( $2p_{3/2}$ ) line from the thio-diluted samples appears at 161.9 eV (associated with thiocarboxylate/carboxylate pairs), while in the thio-rich samples it is at 162.5 eV (attributed to the statistically favored pairs thiocarboxylate/thiocarboxylate). After sulfidization, two sulfur lines at 161.4 (CdS particle associated) and 162.5 eV [ $-C(O)SCd-$  bonds], are detected from both thio-diluted and thio-rich samples; however, with varying relative intensities. This is an important proof for the thioalkanoates as site-directing nucleation centers for CdS. Finally, as already mentioned above, a signal at 163.8 eV was observed from the thio-rich sample, assigned to the  $-C(O)S-H$  bonds created during the sulfidization.

Before reaction with  $H_2S$ , the Cd ( $3d_{5/2}$ ) line of the thio-rich samples appears around 405.6 eV, slightly higher than the Cd of pure carboxylates (405.45 eV). It is noted that a similar analysis of the thio-diluted Cd signal is meaningless, as the unresolved thiocarboxylate related signal is too small. After sulfidization, the line of the thio-rich samples is slightly shifted to 405.4 eV, a value differing more distinctly from that of the pure carboxylates after reaction (405.05 eV).

Finally, the O (1s) signal of thiocarboxylate  $[-C(O)-S^-]$  appears at 532.0 eV before reaction and at 531.5 and 532.0 eV after reaction. The first value agrees with the expected chemical C=O bonds, indicating that the Cd ions bind preferentially to the sulfur atoms, in full agreement with the FT-IR measurements. The 531.5 eV signal is related to the intermediate bonding states, such as  $-C-O-Cd-S$ , at the surfaces of the CdS particles formed within the organic matrices.

The above results can also be interpreted in terms of "core" and "surface" signals corresponding to the various types of CdS particles. "Core" signals are extracted from the Cd and S lines via comparison with reference CdS samples. The ratios of Cd and S ions residing within the cores vs those located at the surfaces of the CdS particles, for  $C_{22}$  alkanoate and thioalkanoate with different compositions, are given in Table 3. The surface-related Cd and S signals are found at positions consistent with Cd-O and/or S-C bonds, where their relative magnitude varies

considerably with increasing concentration of the thioalkanoate, in close agreement with the corresponding changes of the CdS particle sizes deduced independently by other techniques. In fact, by increasing the thioalkanoate concentrations in the mixed crystals, the particles are found to be so small that almost 90% of their atoms are located at the surface. These results are in agreement with the spectroscopic measurements.

### Conclusions

In the present study we demonstrate a successful application of topotactic gas/solid reactions for the preparation of CdS quantum particles arranged in patterns within organic matrices. The key step in such transformations is the ability to control the diffusion of the inorganic particles and sites where they nucleate and grow. Diffusion of the product molecules within the crystallites is anisotropic. In the present class of materials, control on the spacing that separates the ion layers within the reactant materials is achieved by selecting alkanic acids with appropriate chain lengths. With the assistance of the Cd thioalkanoates as site-directing nucleation centers, it became possible to improve the organization of the nanoparticles even in crystals with shorter hydrocarbon chains, as well as to reduce their overall sizes. The homodispersity of the particles is moderate, but there is still room for further improvements. The present method was also successfully applied for the organiza-

tion of the CdS quantum particles within LB films of cadmium alkanates.

TEM studies have also shown that in samples of micron size dimensions, these topotactic reactions occur via single-crystal to single-crystal transformations. In principle, if this tendency could be expressed in systems that display related chemical behaviors, but in addition yield large single crystals, the present method is expected to be useful for the preparation of single crystalline composites that might display interesting anisotropic optoelectronic properties.

Site directing nucleation should be general and applicable for the preparation of other composites with other patterns. The exploitations of unique optoelectronic properties of such systems are currently being studied, and the results will be presented in following publications.

**Acknowledgment.** We thank the Petroleum Research Funds of the American Chemical Society, the Levine funds at the Weizmann Institute of Science, and the Israeli Ministry of Science for Financial support. L.K. thanks the Campomar Foundation and the G.M.J. Schmidt Minerva Center for a fellowship. We also acknowledge Ms. Edna Shavit for synthesis of the thioalkanoic acids and Prof. Leslie Leiserowitz and Dr. Isabelle Weissbuch for fruitful discussions.

JA991354X